American Mineralogist, Volume 91, pages 762–771, 2006

The effect of sodium on the solubilities of metals in silicate melts

ALEXANDER BORISOV,[1,3,*] YANN LAHAYE,[2] AND HERBERT PALME[3]

[1]Institute of Geology of Ore Deposits, Petrography, Mineralogy, and Geochemistry Russian Academy of Sciences, Staromonetny 35, 109017 Moscow, Russia
[2]J.W. Goethe-Universität, Institut für Mineralogie (Abt. Petrologie und Geochemie), Senckenberganlage 28, 60054 Frankfurt, Germany
[3]Universität zu Köln, Institut für Geologie und Mineralogie, Zülpicher Strasse 49b, 50674 Köln, Germany

ABSTRACT

We have studied experimentally the effects of variable Na_2O concentrations on the solubility of four metals (Fe, Co, Ni, and Pd) in silicate melts of anorthite-diopside eutectic composition. Experiments were done at fixed temperatures of 1300 °C for Pd and 1400 °C for Ni, Co, and Fe. In the Fe solubility experiments, Na losses were severe. Therefore, a new experimental device (crucible-supported loop technique or CSLT) was designed to prevent Na losses of experimental charges primarily for experiments at low oxygen fugacities. The CSLT was tested extensively, and it was demonstrated that high Na partial pressures could be kept in a semi-closed crucible for at least 20 h. In experiments on Co solubilities, the CSLT was tested with reversed experiments.

The Fe and Co solubilities clearly decrease with increasing Na_2O contents. The Ni solubility is independent of Na_2O contents up to 4.5 wt%. At oxidizing conditions, a small decrease in Ni solubility with increasing Na content was found. Palladium shows a mixed behavior, decreasing solubility with increasing Na_2O, up to about 4 wt%. At higher Na contents, Pd solubility is independent of Na content.

The increase of FeO activity coefficients with increasing Na content found in this study may provide an explanation for decreasing FeO with decreasing degrees of partial melting in experimentally produced mantle melts (Hirschmann et al. 1998), as melts at low melting degrees are Na-rich.

Keywords: Melt properties, new technique, thermodynamics, experimental petrology

INTRODUCTION

Silicate melts play an important role in geophysics and geochemistry. The structure of volcanic eruptions, and the temporal and areal extent of lava flows depend on the physical properties of the erupting melts, such as viscosity and density. These parameters depend in turn on the chemical composition of the melts. The well-known increase of viscosity with increasing SiO_2 contents reflects the tendency of the melt structure to form a continuous network of $(SiO_4)^{4-}$ tetrahedra. Other components also influence the properties of silicate melts, depending on their structural position in the melt. Some elements, such as Al, support the formation of a continuous network of tetrahedra by replacing Si; other elements, such as Mg and Na, occupy octahedral positions modifying the continuous framework of $(SiO_4)^{4-}$ and $(AlO_4)^{5-}$ tetrahedra. There is, at present, no single theory that provides a quantitative prediction of the physical properties of silicate melts (e.g., melting point and rheology) as function of chemical composition, although attempts to connect the structure, composition, and properties of silicate melts are numerous (e.g., Stebbins et al. 1995).

The sequence of solidification and crystallization of molten silicates, and the composition of the crystallizing minerals, depend on the composition of the melt, more specifically on the thermodynamic activities of the various melt species. There have been considerable efforts to study activities of melt species as function of melt composition (e.g., Ryerson 1985). Holzheid et al. (1997) found that the activities of NiO, CoO, and FeO in silicate melts are largely independent of the chemical composition of the melt. On the other hand, the activity of MoO_2 and MoO_3 in silicate melts is strongly dependent on melt composition (O'Neill and Eggins 2002). Other elements show a more complex behavior (Hess 1995). Our knowledge is, however, restricted to a few elements and the understanding of even these data is still rudimentary.

During the last 10 years, it has become clear that noble metals are, like less noble metals, largely dissolved as oxides in silicate melts (e.g., Borisov and Palme 2000). Nobel metals, such as Pd, follow the same trends as the non-noble metals Ni and Fe. Borisov et al. (2004), for example, found that solubilities of Pd, Ni, and Fe in silicate melts of An-Di-TiO_2 compositions increase with TiO_2 contents at fixed temperature and oxygen fugacity, demonstrating the general similarity in the behavior of noble metals and iron-group metals.

Of some interest is the role of Na in silicate melts, as the Na content of terrestrial magmas is quite variable and its structural role in melts is not well understood. There is, for example, a strong influence of Na and K on the activity of TiO_2 in silicate

* E-mail: aborisov@uni-koeln.de

0003-004X/06/0506–762$05.00/DOI: 10.2138/am.2006.1977

melts (Hess 1995). Some authors believe that the addition of Na to silicate melts would significantly influence the distribution of Fe and Mg between melt and olivine. It has been suggested that the partition coefficient, K_D [= $(Fe/Mg)_{olivine}/(Fe/Mg)_{melt}$], decreases with increasing Na in silicate melts relative to the "classic" value of 0.3 (e.g., Baker et al. 1995, 1996; Falloon et al. 1996, 1997; Draper and Green 1999, etc). There are, however, no *direct* experimental data on the influence of increasing Na contents on K_D. The main reason is the loss of Na in open systems where the oxygen fugacity is imposed by a gas mixture (e.g., Donaldson et al. 1975; Corrigan and Gibb 1979). Similarly, there are no data on the influence of K_2O on FeO and MgO partitioning, excluding, perhaps, the restricted data of Takahashi (1978) in simple model melts. Potassium oxide is even more volatile than Na_2O, and experiments are expected to be even more difficult.

The addition of Na is known to affect the structure of silicate melts (e.g., Mysen and Frantz 1993) as, for example, recorded in the dependence of the Fe^{3+}/Fe^{2+} ratio on the Na_2O content of silicate melts (e.g., Paul and Douglas 1965). Some authors assume a strong effect of alkalis on the silica content of mantle melts (e.g., Hirschmann et al. 1998).

Several attempts to reduce alkali losses from experimental charges are described in the literature. Lewis et al. (1993) placed a crucible with NaCl at the bottom of the furnace to prevent Na losses from experimental charges. In their studies of K solubility in silicate melts, Georges et al. (2000) used a mixture of K_2CO_3 and graphite to produce a constant K vapor pressure in the furnace, and thus, prevent loss of K from the experimental charge. In a recent paper, O'Neill (2005) suggested that the Na vapor pressure could be controlled by hanging an open Pt crucible containing an Na_2O-SiO_2 melt several centimeters beneath the charges. All these techniques lead to extensive contamination of the furnace with Na or K, respectively.

In this paper, we show that at oxidizing conditions, Na losses can be minimized by carefully adjusting the experimental parameters. At reducing conditions, Na losses are, however, so severe that conventional techniques cannot be applied. We thus have developed a new method to maintain a high Na vapor pressure in the furnace close to the location of the loop with silicate melt. The device is tested, and the first results are presented.

Experimental procedures

Most of the experiments were conducted with the conventional loop technique, i.e., by equilibrating metal loops with silicate powder of the desired compositions in a one atm vertical tube furnace under controlled oxygen fugacities (uncertainties of cited log f_{O_2} values and temperature normally do not exceed ±0.1 and ±2 °C, respectively).

The metal bands for the loops were cut from Pd, Ni, Co, or Fe foils (0.1 mm thick, purity of metals >99.95% pure, Chempure). The diameter of the loops was about 2.5 mm.

A synthetic Fe-free melt of anorthite-diopside eutectic composition (DA) was chosen as the basis for silicate compositions. Appropriate amounts of Na_2CO_3 were added to this composition to obtain mixtures with about 1.5 (DAN2), 4.3 (DAN4), 8.4 (DAN8), and 17.3 (DAN17) wt% of Na_2O.

Up to five samples with different Na_2O contents were simultaneously put into the furnace at a given temperature and oxygen fugacity. The Pd solubility was studied at 1300 °C, whereas the Ni, Co, and Fe solubility experiments were done at 1400 °C. After the experiments, samples were quenched by quickly withdrawing the sample holder from the hot zone and moving it to the top of the furnace. Samples were then mounted in epoxy and polished.

Attempts were made to reduce Na losses in the conventional experimental set-up. The total linear velocity of the buffering gas mixture was reduced in most runs to about 0.3 cm/s (at room temperature and atmospheric pressure), three times below the widely adopted value of 0.9 cm/s (Darken and Gurry 1945). Experiments with the so-called "mechanically assisted equilibration technique" (Dingwell et al. 1994), which employ large metal containers enclosing silicate melts, are reported to have used similarly low gas velocities for thousands of hours. Ertel et al. (1996, p. 1173) pointed out "the lack of any significant perturbation of the f_{O_2} as monitored by the oxygen sensor" at a linear gas velocity of 0.3 cm/s.

We used two furnaces in this study, both equipped with electronic mass-flow controllers. The Pd solubility experiments at relatively high f_{O_2} were all done in the same furnace in which f_{O_2} values were controlled by a solid electrolytic cell. The Fe, Co, and Ni solubility experiments were done at much lower oxygen fugacities in a second furnace, and here the f_{O_2} values were calculated from known CO_2/CO gas ratios, as high Na vapor pressures would have damaged the f_{O_2} sensors at low f_{O_2}. To test the f_{O_2} provided by gas mixing independently, the following procedure was adopted. After the experiments with Na-rich melts, the sample-free furnace was equipped with a solid electrolytic sensor. Then, a thermocouple was calibrated against the Ni melting point (1453 °C), the furnace temperature was fixed at 1400 °C, and oxygen fugacities of the same gas mixtures that were earlier used in the Ni, Co, and Fe solubility experiments were checked with the sensor. In this way, we checked the T-f_{O_2} conditions of most Ni, Co, and Fe solubility experiments. A comparison of measured f_{O_2} (no sample in furnace) and calculated f_{O_2} (from CO/CO_2-mixing with Na-rich sample in furnace) is given in Table 1. The difference among the f_{O_2} values is close to zero, and only for the most reducing conditions (2.6% CO_2 in mixture) it reaches 0.16 log units. In conclusion, we are confident that the f_{O_2} calculated from CO/CO_2 mixing is reliable.

To further minimize Na losses, we restricted the duration of the runs at 1400 °C to 4 h, as Borisov (2001) had shown that this is sufficient for equilibrating silicate melts of DA-compositions with Ni loops. However, it appears that the Fe and Co solubility experiments require somewhat longer durations to equilibriate, based on time-series experiments.

Despite these efforts, Na losses from Fe-containing experiments were in all cases severe (see below). We therefore designed a new experimental set-up to maintain a high Na vapor pressure in the gas phase. The principal components of the crucible-supported loop technique (CSLT) are shown in Figure 1. A metal loop with the melt of interest was placed in a small quartz crucible (9.3 mm inner diameter, 20 mm high) containing the Na-rich melt. The crucible was covered with a lid with two holes for fixing the metal loop inside the crucible and to enable to the furnace gas mixture to enter the crucible. Heating of the Na-rich melt during experiments produces a local Na-rich vapor pressure, to which the loop sample is exposed, thus precluding Na evaporation from the sample. In our experiments, we used a glass from laboratory stocks close in composition to sodium disilicate as the Na-carrier (for details of preparation see Courtial et al. 1999). In initial experiments, we used up to 1 g of the Na-bearing glass. As a result, a thin film of melt covered the walls of the crucible and also contaminated the lid. In further experiments, the procedure was standardized as follows: 0.50 ± 0.01 g of the Na source glass powder was put into the crucible and pre-melted in air at 980 °C for 10–20 min. The metal loop was fixed in the crucible below the Pt lid, and the crucible was put into the furnace at the desired T-f_{O_2} conditions. Although premelting of the quartz crucible often produced visible cracks in the crucible, all crucibles survived the experiments without major damage.

In Co solubility experiments, we estimated the furnace contamination with Na by placing an additional, Na-free sample outside the crucible approximately 1 cm away. Both samples, inside and outside the crucible, were equilibrated during

Table 1. Comparison of calculated and measured f_{O_2} values for conditions corresponding to Fe, Co, and Ni solubility experiments

CO_2/CO mL/min	Velocity* cm/s	% CO_2 in mixture	log f_{O_2} calcul.	EMF mV	log f_{O_2} sensor	Comment
457/43	0.295	91.40	–6.56	486.5	–6.54	Ni solubility
420/70	0.289	85.71	–7.06	529.4	–7.06	Ni solubility
340/160	0.295	68.00	–7.96	605.3	–7.97	Ni solubility
200/300	0.295	40.00	–8.97	690.0	–8.99	Co solubility
100/400	0.295	20.00	–9.82	759.5	–9.83	Co solubility
50/450	0.295	10.00	–10.52	815.7	–10.51	Co solubility
30/470	0.295	6.00	–11.00	851.8	–10.94	Co solubility
13/487	0.295	2.60	–11.76	906.0	–11.60	Ni, Fe solubility

Note: All measurments were done at 1400 °C.
* Linear velocity of the buffering gas mixture at room temperature and atmospheric pressure.

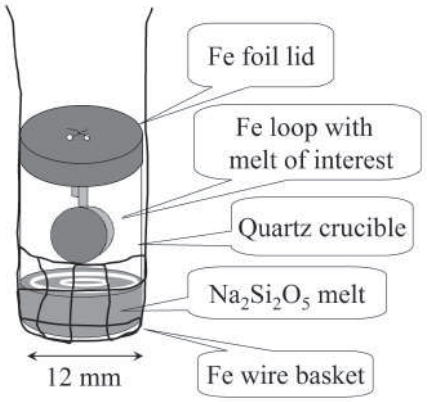

FIGURE 1. Details of the crucible-supported loop technique (CSLT) described in this paper. The crucible shown is designed for the study of Fe solubility. For the Co experiments, the crucible cover and wire basket are made of Pt.

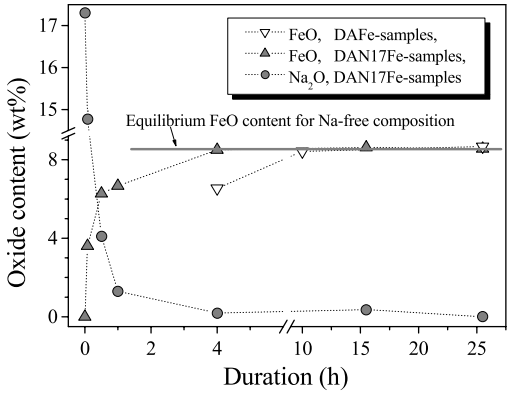

FIGURE 2. Dependence of FeO content in Na-free (DA) and Na-rich (DAN17) melts vs. experiment duration and decrease of Na_2O in initially Na-rich samples (DAN17) with time. Sodium-free samples require significantly more time for equilibration than Na-rich samples (see text for details).

a single run.

Reversals were done in the following way: a somewhat larger quartz crucible (15.0 mm inner diameter, 22 mm high) was loaded with one gram of the Na source glass. Three different samples, Co-free and Na-free, Co-rich and Na-free, and Co-free and Na-rich, were simultaneously put into the crucible and equilibrated for 20 h.

After the experiments, crucibles were split lengthwise in most cases, and the source glass was analyzed by EMP along profiles across the whole crucible.

Bulk compositions of experimental glasses as well as Ni, Co, or Fe contents of silicate glasses were determined by EMP using a JEOL Superprobe (Universität zu Köln, Institut für Geologie und Mineralogie). Natural albite, corundum, and diopside, and metallic Ni, Co, and Fe were used as standards. Operating conditions were 15 kV accelerating voltage, a beam current of 15 nA, and 20 s counting times. Silicate samples produced at very reducing conditions with Ni contents of about 200 ppm were analyzed with a beam current of 500 nA and 200 s counting time. To avoid Na losses under the electron beam, Na-containing glasses were analyzed with a beam diameter of 10 µm. At least seven points were analyzed in each sample and the data were averaged. We used ZAF corrections.

The hydroscopic high-Na source glasses were polished with alcohol and analyzed with a beam diameter of 20 µm and a counting time of 6 s. At least 40 points were analyzed.

The Pd contents of experimental glasses were analyzed by Laser ablation ICP-MS at the Institut für Mineralogie (J.W. Goethe-Universität, Frankfurt), using a Merchantek LUV213 petrographic ultraviolet Nd-YAG laser microprobe coupled with a Finnigan MAT ELEMENT2 high-resolution ICP double-focusing mass spectrometer. The analytical procedure was similar to that described by Borisov et al. (2004). The laser was run at a pulse frequency of 10 Hz and a pulse energy of 1 mJ for a 60 µm spot size. For a 20 µm crater, the pulse frequency was increased to 20 Hz, while the pulse energy was decreased down to 0.25 mJ. The experimental glasses MP12 and MP3 with known Pd contents (INAA, Borisov et al. 1994) were used as external Pd standards. Both standard are free of nanonuggets, as demonstrated by smooth and constant ablation signals.

RESULTS AND DISCUSSION

The Ni-, Co-, and Fe-containing glasses are dark green, dark blue, and aquamarine, correspondingly. All Pd-bearing glasses are transparent, from yellowish to colorless.

Experimental conditions and results of Fe, Co, Ni, and Pd solubilities are given in Tables 2 and 3.

Fe solubility in silicate melts

In Figure 2, we have plotted Fe and Na contents of glasses produced in the Fe experiments as a function of run duration. The DAN17 series demonstrates that about 4 h are required to reach FeO saturation. As expected, the equilibrium FeO content of 8.6 ± 0.2 wt% (average of 5 sample ± 1σ) is the same for the initially Na-free DA samples and the initially Na-rich DAN17 samples. Parallel with increasing FeO is a trend of decreasing Na_2O. Experiments that are initially Na-free (DA) require about 10 h to reach equilibrium, compared to 4 h in experiments with Na-containing starting materials (see Fig. 2).

This trend toward longer equilibration times at low Na contents is highlighted in Figure 3, where we have plotted the FeO contents of a series of experiments, all with 4 h run time, against the initial Na_2O contents. The Na_2O contents after the experiments were 0.19 ± 0.01 wt% in all cases. Only the sample with initially 17 wt% Na_2O has reached the equilibrium FeO content in 4 h. The other samples have lower FeO contents, and the lower the initial Na_2O contents, the larger the difference between equilibrium FeO and measured FeO (after 4 h run time). The more Na is lost, the faster equilibrium is achieved.

One possible explanation for this unexpected effect is faster equilibration of Na-rich melts. If increasing Na would lead to decreasing viscosity, then convective mixing would accelerate equilibration (Borisov 2001). As an example, we compared the viscosities in the DA and DAT8 melts, using the model of Bottinga and Weill (1972). We found, however, that the addition of 8 wt% Na_2O to the DA composition would *increase* the melt viscosity by 60%, from 28 to 46 poises at a temperature of 1400 °C. Thus, if viscosity did influence equilibration times, it should have had the opposite effect.

The mechanism of Na evaporation provides another, perhaps more likely, explanation. As shown by Tsuchiyama et al. (1981), Na evaporates from a melt according to the reaction:

$$NaO_{1/2}\ (melt) = Na\ (vapor) + ¼\ O_2\ (vapor) \quad (1)$$

At the melt-metal loop interface, the "excess" oxygen will react with Fe of the loop, and locally produce additional Fe oxide. The FeO-rich melt layer will then be mixed into the melt by convection, and thus, effectively homogenizing the loop melt in FeO. With increasing amounts of evaporated Na, more "excess"

TABLE 2. Experimental conditions, glass composition (wt%) and MeO contents (FeO, CoO, or NiO, wt%) of silicate melts of Di-An eutectic composition with variable Na_2O contents

No.	Sample*	$-\log f_{O_2}$	h†	SiO_2	Al_2O_3	MgO	CaO	Na_2O	(s.d.)	MeO	(s.d.)	Total
						Fe-loop experiments						
1	DAN17Fe-49	11.76	0.1	41.39	12.72	8.71	19.83	14.77	0.12	3.61	0.05	101.02
2	DAN17Fe-50	11.76	0.5	45.40	13.78	9.41	21.38	4.10	0.07	6.27	0.04	100.34
3	DAN17Fe-51	11.76	1.0	46.66	14.08	9.68	21.79	1.30	0.02	6.67	0.05	100.18
4	DAFe-43	11.76	4.0	47.18	14.27	9.81	22.06	0.18	0.02	6.54	0.04	100.06
5	DAN2Fe-43	"	"	47.08	14.21	9.75	21.95	0.20	0.03	6.66	0.05	99.85
6	DAN4Fe-43	"	"	47.18	14.13	9.73	21.84	0.17	0.02	6.92	0.05	99.96
7	DAN8Fe-43	"	"	46.55	14.15	9.75	21.73	0.20	0.02	7.49	0.06	99.87
8	DAN17Fe-43	"	"	46.10	14.01	9.63	21.59	0.19	0.02	8.50	0.07	100.02
9	DAFe-64	11.76	10.0	46.62	14.20	9.59	21.73	0.01	0.01	8.43	0.04	100.57
10	DAN17Fe-48	11.76	15.5	45.74	13.70	9.53	21.33	0.36	0.02	8.63	0.04	99.29
11	DAFe-65	11.76	25.5	46.13	14.02	9.62	21.70	0.00	0.01	8.67	0.03	100.14
12	DAN17Fe-65	"	"	46.28	14.14	9.62	21.80	0.00	0.01	8.56	0.05	100.41
13	DAN8Fe-46c	11.76	4.0	44.48	13.43	9.19	20.69	6.58	0.07	6.04	0.07	100.42
14	DAN17Fe-45c	11.76	4.0	44.09	13.39	9.23	20.79	6.45	0.09	6.22	0.04	100.18
15	DAN4Fe-47c	11.76	6.5	44.41	13.34	9.13	20.64	6.31	0.08	6.16	0.02	99.99
16	DAFe-52c	11.76	14.0	44.76	13.27	9.16	20.69	5.40	0.06	6.76	0.07	100.04
						Co-loop experiments						
17	DACo-81	8.97	16.0	46.97	14.71	9.85	22.07	0.01	0.01	6.77	0.04	100.39
18	DACo-86	8.97	20.0	47.14	14.75	9.85	22.04	0.52	0.03	6.45	0.05	100.76
19	DACo-86c	"		45.07	14.07	9.42	21.06	6.80	0.07	4.81	0.06	101.24
20	DACo-85	9.82	2.0	49.37	15.39	10.23	23.22	0.03	0.02	2.24	0.04	100.48
21	DACo-85R	"		48.91	15.32	10.26	23.01	0.02	0.02	2.98	0.04	100.52
22	DACo-82	9.82	4.0	49.15	15.37	10.22	23.16	0.02	0.02	2.46	0.04	100.37
23	DACo-82R	"		49.12	15.33	10.22	23.12	0.02	0.01	2.74	0.04	100.54
24	DACo-83	9.82	10.0	49.26	15.34	10.19	23.04	0.01	0.01	2.64	0.04	100.47
25	DACo-83R	"		49.13	15.37	10.21	23.11	0.01	0.01	2.68	0.02	100.51
26	DACo-84	9.82	16.0	49.07	15.42	10.26	23.13	0.01	0.02	2.64	0.04	100.53
27	DACo-84R	"		49.18	15.27	10.17	23.01	0.01	0.01	2.71	0.03	100.34
28	DACo-88c	9.82	20.0	46.21	14.37	9.62	21.49	6.89	0.10	1.83	0.03	100.41
29	DACo-88Rc	"		46.34	14.38	9.61	21.50	6.92	0.05	1.87	0.03	100.62
30	DAN17Co-88c	"		46.40	14.48	9.67	21.67	6.80	0.08	1.86	0.03	100.87
31	DACo-87	10.52	20.0	49.75	15.62	10.28	23.43	0.48	0.03	1.13	0.02	100.69
32	DACo-87c	"		46.82	14.59	9.70	21.96	6.94	0.08	0.83	0.02	100.84
33	DAN17Co-89	11.00	9.0	49.66	15.51	10.28	23.32	0.58	0.03	0.70	0.02	100.06
34	DACo-89c	"		46.89	14.57	9.70	21.85	7.12	0.15	0.48	0.02	100.61
						Ni-loop experiments						
35	DANi-69	6.56	14.5	46.64	14.43	9.89	23.20	0.10	0.02	6.29	0.03	100.55
36	DANi-70	6.56	8.0	46.25	14.35	9.88	23.14	0.73	0.03	6.13	0.15	100.48
37	DAN2Ni-70	"	"	46.10	14.33	9.81	23.09	1.31	0.06	5.89	0.14	100.53
38	DAN4Ni-70	"	"	46.51	14.30	9.81	22.94	2.06	0.01	5.63	0.07	101.25
39	DAN17Ni-70	"	"	46.19	14.32	9.83	22.90	2.58	0.04	5.66	0.05	101.48
40	DANi-34	7.06	4.0	48.54	14.41	10.08	22.75	1.07	0.04	3.54	0.09	100.39
41	DAN2Ni-34	"	"	48.12	14.39	9.91	22.68	1.86	0.04	3.71	0.15	100.67
42	DAN4Ni-34	"	"	47.67	14.26	9.76	22.35	3.04	0.04	3.55	0.03	100.63
43	DAN8Ni-34	"	"	46.84	13.94	9.61	22.11	4.36	0.08	3.44	0.09	100.30
44	DAN17Ni-34	"	"	46.92	13.92	9.66	22.14	4.40	0.05	3.69	0.24	100.72
45	DANi-73	7.06	15.0	48.62	14.95	10.21	23.88	0.05	0.01	3.52	0.03	101.24
46	DANi-74	7.06	8.0	48.51	14.96	10.16	23.83	0.61	0.02	3.42	0.05	101.48
47	DAN2Ni-74	"	"	47.87	14.87	10.15	23.62	1.26	0.04	3.37	0.08	101.15
48	DAN4Ni-74	"	"	47.74	14.80	10.08	23.58	1.79	0.05	3.36	0.13	101.35
49	DAN17Ni-74	"	"	47.58	14.78	10.09	23.63	1.84	0.05	3.37	0.15	101.29
50	DANi-31	7.37	4.0	49.85	15.09	10.46	23.23	0.00	0.00	2.31	0.06	100.93
51	DANi-32	7.37	4.0	49.05	14.76	10.19	22.82	0.17	0.03	2.22	0.02	99.21
52	DAN2Ni-32	"	"	49.38	14.72	10.26	22.98	1.12	0.04	2.27	0.07	100.72
53	DAN4Ni-32	"	"	49.85	14.90	10.43	23.13	1.93	0.05	2.17	0.03	102.41
54	DANi-35	7.61	4.0	48.81	14.75	10.03	22.96	2.03	0.05	1.85	0.08	100.43
55	DAN2Ni-35	"	"	48.77	14.68	10.10	22.88	2.25	0.07	1.86	0.10	100.54
56	DAN4Ni-35	"	"	48.22	14.52	9.98	22.58	2.81	0.05	1.74	0.06	99.85
57	DAN8Ni-35	"	"	48.28	14.50	9.98	22.66	2.71	0.03	1.69	0.03	99.82
58	DAN17Ni-35	"	"	47.53	14.43	9.89	22.54	4.28	0.09	1.92	0.03	100.59
59	DANi-36	7.96	4.0	49.08	14.74	10.11	22.97	1.76	0.06	1.20	0.04	99.86
60	DAN2Ni-36	"	"	48.99	14.64	10.12	22.99	2.05	0.04	1.25	0.04	100.04
61	DAN4Ni-36	"	"	48.70	14.54	10.01	22.87	2.79	0.07	1.29	0.05	100.18
62	DAN8Ni-36	"	"	48.16	14.40	9.99	22.79	2.65	0.05	1.19	0.05	99.18
63	DAN17Ni-36	"	"	47.84	14.35	9.96	22.79	3.48	0.06	1.39	0.03	99.80
64	DANi-71	7.96	18.0	49.81	15.37	10.34	24.44	0.05	0.02	1.29	0.06	101.29
65	DANi-72	7.96	8.0	49.32	15.23	10.33	24.25	0.59	0.02	1.27	0.01	100.98
66	DAN2Ni-72	"	"	49.11	15.21	10.36	24.24	0.91	0.02	1.24	0.04	101.06
67	DAN4Ni-72	"	"	49.01	15.14	10.27	24.22	1.17	0.02	1.27	0.02	101.08
68	DAN17Ni-72	"	"	48.73	15.13	10.49	24.23	0.87	0.03	1.27	0.02	100.71
69	DANi-67	11.76	8.0	50.78	15.42	10.54	23.75	0.01	0.01	0.0205	0.0023	100.53
70	DAN2Ni-67	"	"	50.65	15.38	10.58	23.97	0.01	0.01	0.0205	0.0013	100.60
71	DAN4Ni-67	"	"	50.52	15.28	10.53	23.95	0.01	0.01	0.0205	0.0006	100.31
72	DAN8Ni-67	"	"	50.56	15.25	10.53	23.94	0.01	0.01	0.0207	0.0013	100.31

* All experiments were done at 1400 °C; *c* = CSL Technique, *R* = reversal, that is a sample with initially high CoO content (6.8 wt%); f_{O_2} values were calculated from CO/CO_2 ratios and later checked with a sensor (see Table 1); s.d. = standard deviation. † Duration of experiment in hours.

TABLE 3. Experimental conditions, glass composition (wt%) and Pd contents (ppm) of silicate melts of Di-An eutectic composition with variable Na_2O contents

No.	Sample	$-\log f_{O_2}$	*h	SiO_2	Al_2O_3	MgO	CaO	Na_2O	(s.d.)	Pd	(s.d.)	Total
1	DA-29	0.68	48.0	50.92	15.21	10.55	23.60	0.30	0.04	276.8	10.4	100.57
2	DAN2-30	0.68	25.0	50.49	15.09	10.39	23.41	1.44	0.05	251.6	9.5	100.82
3	DA-25	0.68	40.0	50.07	15.27	10.38	23.17	2.06	0.06	249.7	9.6	100.95
4	DAN2-25	"	"	49.3	14.97	10.18	22.70	3.75	0.08	218.9	8.6	100.91
5	DAN4-25	"	"	48.62	14.74	10.02	22.51	5.10	0.11	246.8	9.9	100.99
6	DAN8-25	"	"	47.59	14.39	9.82	21.98	7.29	0.11	245.8	10.2	101.06
7	DAN17-25	"	"	46.58	14.49	9.83	21.82	8.43	0.09	232.3	9.9	101.15
8	DA-26	3.08	40.0	50.59	15.52	10.55	23.55	0.70	0.06	42.19	1.92	100.91
9	DAN2-26	"	"	50.24	15.25	10.4	23.18	2.28	0.08	38.81	1.82	101.35
10	DAN4-26	"	"	49.07	15.06	10.26	22.63	4.43	0.06	29.80	1.46	101.45
11	DAN17-26	"	"	45.86	14.11	9.54	21.31	11.09	0.12	30.73	1.56	101.91
12	DAN17-8	10.46	7.0	48.46	15.13	10.34	22.59	4.26	0.07	0.666	0.087	100.78
13	DAN17-10	10.71	7.0	49.69	15.20	10.27	22.89	3.50	0.13	0.592	0.032	101.55
14	DAN17-9	10.91	6.0	48.61	15.07	10.28	22.71	4.15	0.06	0.543	0.013	100.83
15	DAN17-14	11.23	6.0	49.72	15.47	10.57	23.20	2.58	0.08	0.448	0.013	101.54

Notes: All experiments were done at 1300 °C; f_{O_2} values were measured by oxygen sensor. s.d. = standard deviation.
* Duration of experiment in hours.

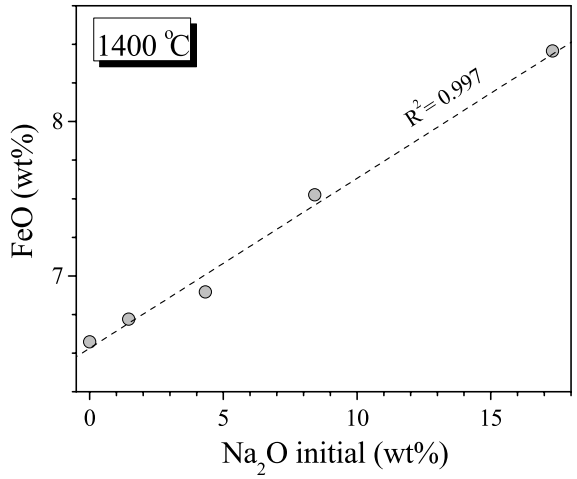

FIGURE 3. Dependence of FeO content in experimental samples vs. initial Na_2O concentration. The Na_2O contents in these glasses after the experiments are in all cases below 0.2 wt%. Loss of Na_2O leads to oxidation of additional Fe (see text for details).

FeO is produced at the surface of the melt approaching the FeO equilibration content reached. Thus, loss of volatile components may provide a means of accelerating reactions occurring at the surface of the melt. This may be particularly important for very viscous silica-rich melts, where the time of metal-melt equilibration experiments will be reduced significantly.

The fast loss of Na at reducing conditions is seen in Figure 2. After 1 h, melt DAT17 has lost 90% of its Na; after 4 h, practically all Na is lost from the initially Na-rich melt. Thus, experiments to determine the Fe solubility in Na-rich melts require a technique that prevents Na loss in one atm experiments, such as the CSLT described in the previous section.

With this set-up, three short runs (4 h) were made with the same composition (DAN4, DAN8, and DAN17), except for variable initial Na_2O contents. The Na_2O melt contents after the experiments were 6.45 ± 0.14 wt% Na_2O, which are identical and independent of the initial Na-contents (Table 2). This finding demonstrates that this technique gives reproducible results and that the Na partial pressure generated inside the crucible defines the Na content in the silicate melt. We also demonstrated that the run duration of 4 h is sufficient to equilibrate the silicate melt with the crucible atmosphere and the enclosing Fe loop, as the Fe content is the same in all three samples (6.14 ± 0.09 wt% FeO), and thus, reflects equilibrium for the Na-containing melts.

A somewhat lower Na-content of 5.40% Na_2O (DAFe-52c, Table 2) was obtained in a 14 h run (see below for details).

If we combine the results of the conventional loop method and the CSLT method, we see a clear decrease in the FeO solubility with increasing Na_2O contents, from 8.56 ± 0.1 wt% for an Na_2O-free melt down to 6.14 ± 0.09 wt% for a melt containing about 6.5 wt% Na_2O (Fig. 4).

Co solubility in silicate melts

The Co solubility experiments were designed to further demonstrate equilibrium in CSLT experiments by doing reversed experiments and to estimate the effects of contamination of the furnace with Na. The conditions of experiments along with the results of CoO contents are given in Table 2.

In a series of conventional loop experiments, including four that were reversed (high initial Co), it was demonstrated that 10 h are sufficient to reach metal/melt equilibrium (Fig. 5). As noted above, we reversed experiments with respect to Co and Na by simultaneously equilibrating three different samples in a single crucible: Co-free and Na-free, Co-rich and Na-free, and Co-free and Na-rich samples. After 20 h, all three samples showed essentially the same Na_2O and CoO contents (6.87 ± 0.06 and 1.85 ± 0.02 wt%, respectively), demonstrating the reliability of the new technique.

The CSL method decreases furnace contamination with Na in comparison with previously suggested methods (Lewis et al. 1993; Georges et al. 2000; O'Neill 2005). The small Na content of initially Na-free samples, equilibrated in the same runs (about 0.5 wt% Na_2O, see Table 2) demonstrates that such contamination cannot be completely excluded. In any case, it is clear that CSLT allows for the study of both Na-free and Na-poor samples.

In Figure 6, we have plotted the equilibrium Co solubility values vs. $\log f_{O_2}$. Lines with the ideal slope of 0.5, representing Co^{2+} as the principal melt species, are also shown. Both Na-rich and Na-poor samples fit the ideal Co solubility precisely, indicating excellent accuracy of the present experiments, including those obtained with the CSLT (marked with letter "c" in Table

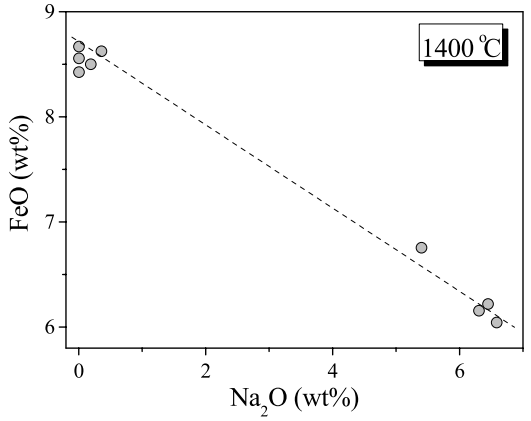

FIGURE 4. Dependence of Fe solubility on Na contents in DA+Na_2O silicate melts.

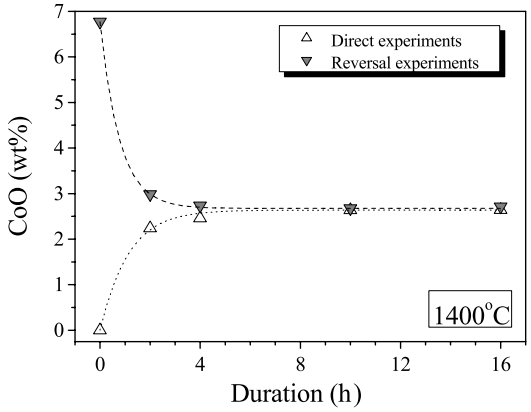

FIGURE 5. Relationship between the CoO contents in initially Co-free (direct experiments) and initially Co-rich DA melts (reversals) and experiment duration. Cobalt-rich sample used for reversal experiments were premelted at more oxidizing conditions and contained 6.8 wt% CoO.

2). There is no doubt that the solubility of Co in Na-rich melts is reduced by some 30% compared to Na-free melts, independent of oxygen fugacity. A fit of the Co solubility data vs. f_{O_2} and Na_2O content yields the following equation ($R^2 = 0.999$):

$$\log C_{CoO}\,(\text{wt\%}) = 0.483 \log f_{O_2} - 0.023 \log C_{Na_2O}\,(\text{wt\%}) \qquad (2)$$

According to this equation, at a given f_{O_2} value an Na_2O content of about 13 wt% would reduce the Co-solubility by a factor of two compared to Na-free melts.

Comments on the crucible supported loop technique

Since experiments with Ni and Pd were done exclusively with the conventional loop technique, we add here some comments on the newly developed method used for Fe and Co. As mentioned above, we used glass powder from the laboratory stocks as an Na source in all experiments, based on the assumption that composition of the glass is very close to Na disilicate (Courtial et al. 1999, Table 1, sample NS2). Indeed, the composition determined after melting in air at 980 °C during 15 min in a Pt loop showed an Na_2O content of 33.9 ± 0.3 wt% (ideal $Na_2Si_2O_5$ contains 34.0

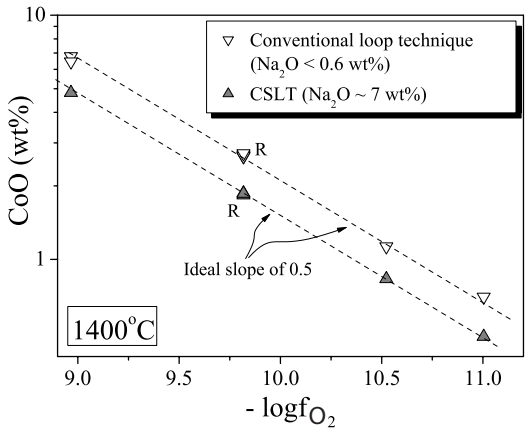

FIGURE 6. Dependence of cobalt solubility in DA+Na_2O silicate melts on f_{O_2}. [*R* indicates reversed experiments with initially high CoO contents (6.8 wt%).] Both Na-poor samples prepared with the conventional loop technique and Na-rich samples (with CSLT) yield nearly the ideal slope of 0.5 characteristic of Co^{2+}.

wt% Na_2O). During an experimental run, this composition should move to the silica-rich side of the Na_2O-SiO_2 phase diagram because of Na losses to the atmosphere and partial dissolution of the crucible walls.

The glasses were found to be slightly heterogeneous, as the Na_2O content in the uppermost 1 mm region (close to the menisci) is on average 2 wt% higher than Na_2O in the lowermost 1 mm region (close to the crucible bottom). Thus, for the purpose of comparing results of different experiments, we have used the average Na_2O content in the uppermost 1 mm of source glass. All measured Na contents in these glasses, including three blank experiments are plotted vs. experimental duration on Figure 7. It appears that the final amount of Na_2O in the source glass is primarily controlled by the duration of the experiment, but not by oxygen fugacity. This finding may indicate that crucible walls dissolution plays a big role in changing of the source melt composition.

Our experience with the CSLT describe above may be summarized as follows: (1) The method works quite well for relatively short runs (several hours) at any low oxygen fugacity. (2) Inert crucible materials other than quartz (e.g., Pt), can be used, although other experimental problems (e.g., very strong melt creep on Pt crucible walls) may arise. (3) At moderately high temperatures (where the liquidus melt in the Na_2O-SiO_2 binary is still relatively Na-rich, say below 1450 °C), the CSLT appears to work for much longer durations. The analysis of the residual Na-rich glass in one experiment at 1400 °C, with 20 h run time and at an f_{O_2} as low as $10^{-10.52}$ atm, gave a silica content of 82.9 wt%, still slightly below the liquidus composition in the Na_2O-SiO_2 binary (86.4 wt% at 1400 °C). After the melt composition has reached the liquidus, SiO_2 will precipitate and the melt composition will not change. Constant composition of the source melt at constant temperature, and oxygen fugacity will lead to constant Na pressure inside the crucible.

Silica evaporation from the source melt and subsequent transfer to the loop melt (as was suggested by one reviewer) was never

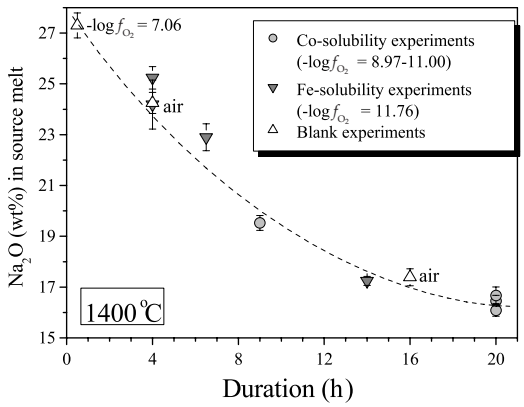

FIGURE 7. Dependence of Na_2O content of the Na source glasses after the experiments vs. experimental duration (see text for details).

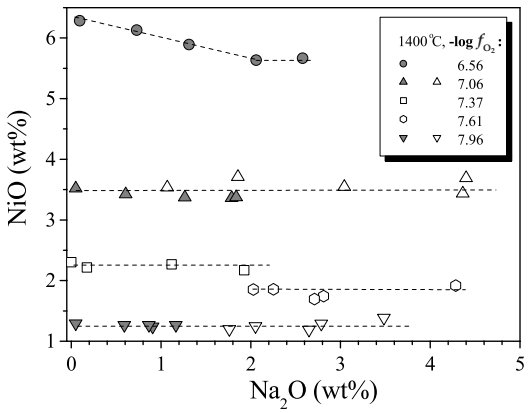

FIGURE 8. Dependence of Ni solubility in DA+Na_2O silicate melts on sodium contents. Results for both "short" (4 h, open symbols) and "long" (8 h or longer, closed symbols) experiments are shown. There is no apparent dependence of dissolved NiO on Na_2O contents of up to nearly 5%.

observed. We recalculated the compositions of all experimentally produced glasses to an Na and metal (Fe, Co, Ni, or Pd)-free base. The silica content in the CSLT experiments (50.5 ± 0.2 wt%, avg. of 10) is equal to the silica contents of conventional loop experiments (50.3 ± 0.4 wt%, avg. of 77).

Another concern raised in review was that the additional O_2 released from evaporation of the Na source melt may enhance the f_{O_2} in the crucible. A comparison of experimental results in systems with and without the CSL technique indicates that such effects are not observed, as may be seen from Figure 6. The high Na-experiments with the new technique and the low Na-experiments with the conventional technique show the same dependence on f_{O_2}, with a slope that reflects the presence of Co^{2+} in the melt, in both cases. If the effective f_{O_2} in Na-rich experiments were higher, due to evaporation of Na, one would expect higher contents of CoO in the melt because of the general increase of Co-solubility with increased f_{O_2}. The opposite is the case: the Co-solubilities in Na-rich experiments are lower than those in Na-poor experiments. There is no indication that evaporation of Na from the Na-source melt has any effect on the effective f_{O_2} established by the CO-CO_2 gas mixture. The experimental results displayed in Figure 6 demonstrate convincingly that the f_{O_2} in the Na-containing crucible can be controlled independently, as seen from the slope of the correlation for Na-rich experiments.

Ni solubility in silicate melts

All Ni solubility experiments were conducted with the conventional loop technique. Most experiments were performed at values of f_{O_2} significantly above those used in the Fe solubility experiments, and consequently Na losses were smaller. In Ni experiments at low f_{O_2} values similar to those in the Fe experiments, Na_2O was lost quantitatively, not unlike Fe at these conditions. Initial runs with Ni were comparatively short (about 4 h), based on the conclusion of Borisov (2001) that this time is sufficient to equilibrate DA composition with Ni metal at 1400 °C. In addition, Na losses would be kept to a minimum. It was later found, however, that 4 h are not sufficient to equilibrate Na-free and Na-poor samples with Fe or Co loops. Therefore, several runs of 8 h or longer duration were performed. All experimental results are given in Table 2. Results (excluding those at the lowest f_{O_2} of $10^{-11.76}$ atm, which have lost all Na) are graphically displayed in Figure 8.

In several runs, Na-rich and Na-poor or Na-free samples were placed into the furnace simultaneously. Evaporation of Na from the Na-rich samples led to an increase in the local partial pressure of Na in the furnace atmosphere and the Na-free or Na-poor samples acquired Na. Thus, some samples have higher Na after the experiment than before (see Nos. 40, 46, 54, 55, 59, 60, and 65 in Table 2).

Figure 8 demonstrates that at constant f_{O_2}, the increase of Na_2O up to 4.2% has no effect on the Ni solubility, quite different from the effect of Na on Fe and Co solubilities. Only at the most oxidizing conditions ($10^{-6.59}$ atm) does an Na_2O increase from zero to 2.06 wt% result in a slight decrease of dissolved NiO, from 6.3 to 5.6 wt% NiO (see Fig. 8).

We fitted the Ni solubility data (including data at $10^{-11.76}$ atm, which are not shown in Fig. 8) as functions of f_{O_2}. The slope of the correlation of log NiO vs. log f_{O_2} (0.473 ± 0.002, R^2 = 0.999) is close to the theoretical value of 0.5, as expected for Ni^{2+}. This excellent correlation demonstrates the accuracy of the results, and indicates that equilibrium has been achieved in all experiments.

Pd solubility in silicate melts

The first results on the effect of Na on Pd solubility in silicate melts were obtained as a by-product of a project to study the effect of Na on silica activity in silicate melts. In these experiments, Na-free (DA) and Na-rich (DAN17) melts were equilibrated with Pd metal loops, and the Si content of the Pd metal was determined. Following the idea of Chamberlin et al. (1994), these Si contents might be converted to the SiO_2 activities of the silicate melt. The glasses produced in these experiments were then analyzed for Pd by LA ICP-MS.

Many of the samples studied in the present work were contaminated with tiny metal nuggets (e.g., Borisov et al. 2004). Only four samples with 2.6 to 4.3 wt% Na_2O contained areas free of nuggets that were suitable for analyses with a 30 µm laser beam. The results are given in Table 3, and are also shown

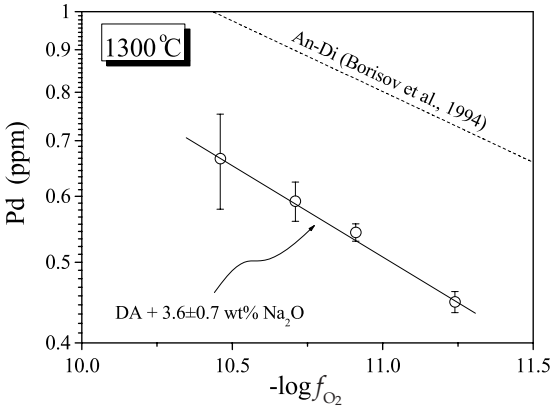

FIGURE 9. Dependence of Pd solubility in DA+Na_2O silicate melts on f_{O2}. Earlier results in Na-free DA melts (Borisov et al. 1994) recalculated to the same temperature are also shown. The solubility of Pd in Na-containing melts is apparently lower than in Na-free melts.

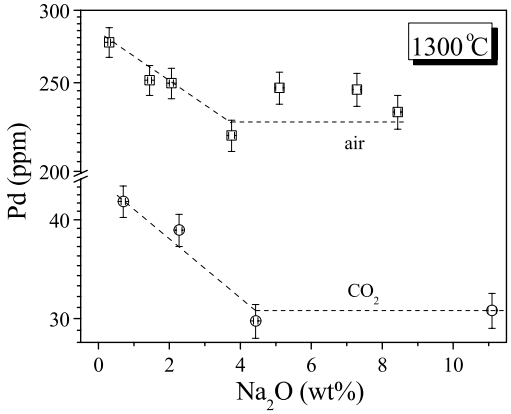

FIGURE 10. Dependence of Pd solubility in DA+Na_2O silicate melts on the Na contents at two different values of f_{O2}.

in Figure 9, where Pd concentrations are plotted against log f_{O_2}. Previous results on Pd solubility in Na-free melts (Borisov et al. 1994) have been recalculated to the same temperature and are also shown. Systematic differences between the two series of Pd-analyses were eliminated by using a sample from the Borisov et al. (1994) data as a standard for Pd-analyses in the present study. Thus, the reduction in Pd solubility by the addition of Na is not an experimental artifact.

Subsequently two additional series of experiments were conducted at a fixed temperature of 1300 °C and at oxidizing conditions (air and pure CO_2) where nugget formation is known to be small. The Na_2O content of the silicate melt was the only variable. The results of these experiments are listed in Table 3, and are displayed graphically in Figure 10. Addition of up to 4 wt% Na_2O has a pronounced effect on the Pd solubility, resulting in a 20–30% decrease of Pd contents at fixed temperature and oxygen fugacity. Further addition of Na_2O does not affect the solubility of Pd.

NiO, CoO, and FeO activities in silicate melts: effects of melt composition and comparison with published data

The equilibrium of metallic Ni, Co, or Fe with silicate melts may be described by the reaction:

$$\text{Me (metal)} + 1/2\ O_2 = \text{MeO (silicate melt)} \quad (3)$$

where Me is Ni, Co, or Fe, and MeO is NiO, CoO, or FeO, correspondingly. The MeO activity coefficients are then described as:

$$\log \gamma_{MeO} = -\Delta G_3/2.303RT - \log X_{MeO} + 1/2 \log f_{O_2} \quad (4)$$

where ΔG_3 is the free energy of the reaction 3 at temperature T, and X_{MeO} is the mole fraction of metal oxide in the silicate melt. We followed the procedure of Holzheid et al. (1997) and O'Neill and Eggins (2002) to use liquid NiO, CoO, and FeO as standard states for calculating the activity coefficients. This choice minimizes the temperature dependence of the activity coefficients.

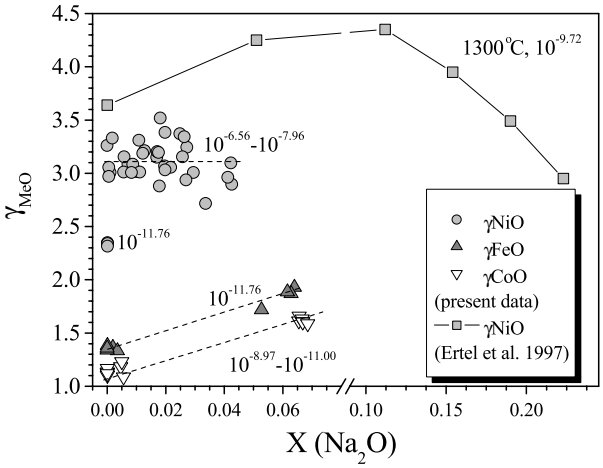

FIGURE 11. Dependence of NiO, CoO, and FeO activity coefficients in DA+Na_2O silicate melts on Na_2O in melts at 1400 °C. The Ertel et al. (1997) data were obtained at a different temperature (1300 °C) and variable SiO_2-contents (see text for details)

Calculated activity coefficients are plotted in Figure 11, and are compared with literature data.

The γ_{NiO} value of 3.12 ± 0.17 (average of 34 experiments ± 1σ, f_{O_2} from $10^{-6.56}$ to $10^{-7.96}$ atm, percentage-level of Ni in the silicate melt) is within error limits independent of the Na_2O content of the melts. The γ_{NiO} values at the lowest f_{O_2} of $10^{-11.76}$ atm (ppm-level of Ni in the silicate melt) cluster around 2.34 ± 0.01 (average of four samples). It is possible that Henry's Law is not valid for the high-NiO experiments. Also, small systematic errors in analytical procedures cannot be excluded, as the Ni contents in the reducing experiments are in the ppm levels.

Literature values for γ_{NiO} at conditions similar to those applied here cover a comparatively large range: 2.34 ± 0.01 (present data, microprobe), 2.52 (O'Neill and Eggins 2002, LA ICP-MS), 2.91 ± 0.56 (Holzheid et al. 1997, INAA), and 3.0 (Ertel et al. 1997, ICP-AES). These variations indicate that interlaboratory differences in the experimental determination of activity coefficients, caused by systematic differences in the determination of f_{O_2}, temperature, and MeO content, may be relatively large and do not allow the detection of small effects of melt composition.

To avoid analytical bias, the determination of the dependence of γ_{NiO} on melt composition preferably should be done in a single laboratory.

The only other systematic study of the effect of the addition of Na on the solubility of Ni in silicate melts was done by Ertel et al. (1997) at 1300 °C and at log f_{O_2} = –9.72, using a crucible stirring technique. To minimize Na losses, Na was added to the DA composition as Na_2SiO_3. The Ni content in sampled glasses was analyzed by ICP-AES. These authors found a complex behavior of γ_{NiO}, first an increase from 3.64 for pure DA melt up to 4.35 for DA+23% Na_2SiO_3, and then again a decrease to 2.95 for DA+45% Na_2SiO_3. The effects of Na_2O and SiO_2 in that study cannot be separated easily. On the one hand, Ertel et al. (1997) found no effect of the addition of silica to the DA composition, i.e., the Ni solubility (activity) did not change. On the other hand, O'Neill and Eggins (2002) found at slightly different conditions (1400 °C and at log f_{O_2} = –9.60) that the addition of 50% silica to DA resulted in a decrease of the Ni solubility from 2038 to 1675 ppm (LA ICP-MS data, Table 3 in O'Neill and Eggins 2002). Both results are surprising, considering that SiO_2 is a network-forming oxide, similar to TiO_2, the addition of which was found to increase the solubility of Ni (O'Neill and Eggins 2002; Borisov et al. 2004). Assuming that the solubility of Ni is independent of silica content, the complex behavior of Ni found by Ertel et al. (1997) associated with the addition of Na_2SiO_3 must be entirely due to the behavior of Na in the silicate melt. In Figure 11, we plotted the Ertel et al. (1997) data vs. X_{Na_2O} . The increase of γ_{NiO} with increasing Na (up to about 11 mol%) is similar to what we found for γ_{FeO} and γ_{CoO}, (see below), but differs from our data for γ_{NiO}. The reason for this discrepancy is not clear.

Pretorius and Muan (1992) studied the effects of adding K_2O to CaO-MgO-SiO_2 melts and found that addition of K results in an increase in the activity coefficients of NiO, although O'Neill and Eggins (2002, p. 170) had on the basis of the same data concluded that the effect of K_2O is negligible.

In Figure 11, we have also plotted the activity coefficients of FeO and CoO as obtained in this study. They are, in contrast to γ_{NiO}, dependent on the Na content of the melt. The value of γ_{FeO} increases from 1.36 ± 0.02 (average of 5) for Na-free melts to 1.90 ± 0.03 (average of 3) for melts with about 6.4 wt% Na_2O, and the value of γ_{CoO} increases from 1.13 ± 0.02 (average of 5) for Na-free melts to 1.62 ± 0.03 (average of 6) for melts with about 6.9 wt% Na_2O (see Fig. 11). In an earlier study, Borisov et al. (2004) found that log γ_{FeO} and log γ_{NiO} is a linear function of X_{TiO_2} in melts of DA+TiO_2 composition. O'Neill and Eggins (2002) also pointed out the logarithmic relationship between MoO_2 and MoO_3 activity coefficients and X_{CaO} in silicate melts. Assuming similar dependences for Na_2O, we can write:

$$\log \gamma_{MeO} = k \cdot X_{Na_2O} + A \quad (5)$$

where k and A are constants. The regression of log γ_{FeO} and log γ_{CoO} vs. X_{Na_2O} yields k = 2.29 ± 0.11, and A = 0.13 ± 0.01 for the Fe data (R^2 = 0.985) and k = 2.32 ± 0.12 and A = 0.05 ± 0.01 for the Co data (R^2 = 0.971).

Our γ_{FeO} value of 1.36 ± 0.02 and the γ_{CoO} value of 1.13 ± 0.02 for Na-free melts are in an excellent agreement with γ_{FeO} value of 1.37 and γ_{CoO} value of 1.12 found by O'Neill and Eggins (2002) for the same melt composition and the same temperature. It is worth mentioning that our γ_{CoO} values were derived from melts with CoO of 2–5 wt% Co, whereas O'Neill and Eggins (2002) derived activity coefficients from melts with about 3000 ppm Co, indicating that Henry's Law is obeyed at this range of concentrations.

Doyle (1988) investigated the FeO solubility in relatively simple melts of SiO_2-Al_2O_3-CaO-K_2O composition at 1600 K. We calculated activity coefficients from their solubility data (129 experiments) and performed a regression of log γ_{FeO} vs. X_{K_2O}, assuming that K_2O is the only component affecting γ_{FeO}. As a result, we obtained k = 4.07 ± 0.25 and A = –0.015 ± 0.062 (R^2 = 0.674), indicating an even stronger dependence of the activity of FeO on the K_2O content than for Na_2O. The addition of only 3 mol% K_2O to a K-free SiO_2-Al_2O_3-CaO melt will increase γ_{FeO} from 0.97 to 1.28.

In summary, it appears that the addition of both Na_2O and K_2O will increase the activity coefficients of FeO and CoO in silicate melts, but has no or only a small effect on the activity coefficient of NiO.

We also can estimate the effects of Na on the activity coefficient of MgO in silicate melts. The exchange reaction of Mg and Fe between olivine and melt may be written as:

$$Mg_2SiO_4 \text{ (olivine)} + 2FeO \text{ (melt)} = Fe_2SiO_4 \text{ (olivine)} + 2MgO \text{ (melt)}. \quad (6)$$

Assuming ideal mixing of fayalite and forsterite (e.g., O'Neill et al. 2003), the Mg/Fe olivine/melt partition coefficient (K_D) at can be written as:

$$\log K_D = B + \log \gamma_{FeO} \text{ (melt)} - \log \gamma_{MgO} \text{ (melt)}. \quad (7)$$

By assuming that both γ_{FeO} and γ_{MgO} depend linearly on the Na content according to Equation 5, we obtain:

$$\log K_D = C + (k_{FeO} - k_{MgO}) \cdot X_{Na_2O} \quad (8)$$

where B, C, k_{FeO}, and k_{MgO} are constants.

It is often assumed that high contents of Na in silicate melts significantly decrease K_D relative to the "classic" value of 0.30, although the extent of the deviation from the value of 0.30 is unclear (e.g., Baker et al. 1995, 1996; Falloon et al. 1996, 1997; Draper and Green 1999, etc.). In Equation 8, the difference (k_{FeO} – k_{MgO}) < 0, or $k_{MgO} > k_{FeO}$, which implies a stronger increase of γ_{MgO} than of γ_{FeO} with increasing Na_2O contents.

The influence of Na_2O on the FeO-contents of primary mantle melts

The FeO content of melts in equilibrium with the minerals of the upper mantle of the earth is determined by the activity of FeO, which is defined by the equilibrium of the ferrosilite component of orthopyroxene and the fayalite component of olivine, according to:

$$FeSiO_3 \text{ (orthopyroxene)} + FeO \text{ (melt)} = Fe_2SiO_4 \text{ (olivine)} \quad (9)$$

As the compositions of olivine and pyroxene will not change

with removal of small degrees of partial melts, variations in the FeO contents of partial mantle melts primarily reflect changes in the activity coefficient of FeO in the partial melt, as at nearly constant temperature, the equilibrium constant of reaction 9 and the activity ratio $a_{Fe_2SiO_4}/a_{FeSiO_3}$ are constant. Differences in FeO contents of two melts produced by different degrees of partial melting of two liquids *i* and *j* must reflect differences in the activity coefficients of FeO in the corresponding melts, as $X_{FeO}{}^i/X_{FeO}{}^j = \gamma_{FeO}{}^j/\gamma_{FeO}{}^i$.

The same holds for the Mg contents of primary mantle melts, which are determined by the equilibrium:

$$MgSiO_3 \text{ (orthopyroxene)} + MgO \text{ (melt)} = Mg_2SiO_4 \text{ (olivine)} \quad (10)$$

The FeO content of primary mantle melts at small degrees of melting is variable as, for example shown in Figure 3 of Hirschmann et al. (1998), based on experimental data by Baker and Stolper (1994) and Baker et al. (1995). The increase in FeO (from about 4 wt% at 2% partial melting to about 6 wt% at 5% partial melting) correlates with the decrease in sodium contents from about 7 to about 4 wt%, in qualitative agreement with our finding. The MgO content shows a parallel behavior with a somewhat stronger increase, in agreement with estimates given above.

For a more quantitative treatment, the effects of all other major components as well as the influence of pressure need to be considered. The present data may be considered a first step for a more quantitative understanding of the composition of partial melts in the mantles of the Earth and other differentiated planets.

ACKNOWLEDGMENTS

This study was supported by the Deutsche Forschungsgemeinschaft (DFG) and by the Russian Foundation for Basic Research. The manuscript was considerably improved by comments of Astrid Holzheid, Hugh O'Neill, and Werner Ertel.

REFERENCES CITED

Baker, M.B. and Stolper, E.M. (1994) Determining the composition of high-pressure mantle melts using diamond aggregates. Geochimica et Cosmochimica Acta, 58, 2811–2827.

Baker, M.B., Hirschmann, M.M., Ghiorso, M.S., and Stolper, E.M. (1995) Composition of near-solidus peridotite melts from experiments and thermodynamic calculations. Nature, 375, 308–311.

Borisov, A. (2001) Loop technique: dynamic of metal/melt equilibration. Mineralogy and Petrology, 71, 87–94.

Borisov, A. and Palme, H. (2000) Solubilities of noble metals in iron-containing silicate melts as derived from experiments in iron-free systems. American Mineralogist, 85, 1665–1673.

Borisov, A., Palme, H., and Spettel, B. (1994) Solubility of palladium in silicate melts: implications for core formation in the Earth. Geochimica et Cosmochimica Acta, 58, 705–716.

Borisov, A., Lahaye, Y., and Palme, H. (2004) The effect of TiO_2 on Pd, Ni, and Fe solubilities in silicate melts. American Mineralogist, 89, 564–571.

Bottinga, Y. and Weill, D.F. (1972) The viscosity of magmatic silicate liquids: a model for calculations. American Journal of Science, 272, 438-475.

Chamberlin, L., Beckett, J.R., and Stolper, E. (1994) Pd-oxide equilibration: a new experimental method for the direct determination of oxide activities in melts and minerals. Contributions to Mineralogy and Petrology, 116, 169–181.

Corrigan, G. and Gibb, F.G.F. (1979) The loss of Fe and Na from a basaltic melt during experiments using the wire-loop method. Mineralogical Magazine, 43, 121–126.

Courtial, P., Gottsmann, J., Holzheid, A., and Dingwell, D.B. (1999) Partial molar volumes of NiO and CoO liquids: implications for the pressure dependence of metal–silicate partitioning. Earth and Planetary Science Letters, 171, 171–183.

Darken, L.S. and Gurry, R.W. (1945) The system iron-oxygen. I. The wüstite field and related equilibria. Journal American Chemical Society, 67, 1398–1412.

Dingwell, D.B., O'Neill, H.St.C., Ertel, W., and Spettel, B. (1994) The solubility and oxidation state of Ni in silicate melts at low oxygen fugacities: results using a mechanically assisted equilibration technique. Geochimica et Cosmochimica Acta, 58, 1967–1974.

Donaldson, C.H., Williams, R.J., and Lofgren, G. (1975) A sample holding technique for study of crystal growth in silicate melts. American Mineralogist, 60, 324–326.

Doyle, C.D. (1988) Prediction of the activity of FeO in multicomponent magma from known values in [SiO_2-$KAlO_2$-$CaAl_2Si_2O_8$]-FeO liquids. Geochimica et Cosmochimica Acta, 52, 1827–1834.

Draper, D.S. and Green, T.H. (1999) *P-T* phase relations of silicic, alkaline, aluminous liquids: new results and applications to mantle melting and metasomatism. Earth and Planetary Science Letters, 170, 255–268.

Ertel, W., Dingwell, D.B., and O'Neill, H.St.C. (1996) Solubility of tungsten in a haplobasaltic melt as function of temperature and oxygen fugacity. Geochimica et Cosmochimica Acta, 60, 1171–1180.

——— (1997) Compositional dependence of the activity of nickel in silicate melts. Geochimica et Cosmochimica Acta, 61, 4707–4721.

Falloon, T.J., Green, D.H., O'Neill, H.St.C., and Ballhaus, C.G. (1996) Quest for low-degree mantle melts (Scientific Correspondence). Nature, 381, 285.

Falloon, T.J., Green, D.H., O'Neill, H.St.C., and Hibberson, W.O. (1997) Experimental tests of low degree peridotite partial melt compositions: Implications for the nature of anhydrous near-solidus. Earth and Planetary Science Letters, 152, 149–162.

Georges, P., Libourel, G., and Deloule, E. (2000) Experimental constraints on alkali condensation in chondrule formation. Meteoritics and Planetary Science, 35, 1183–1188.

Hess, P.C. (1995) Thermodynamic mixing properties and the structure of silicate melts. In J.F.Stebbins, P.F. McMillan, and D.B. Dingwell, Eds., Structure, dynamics and properties of silicate melts, 32, p. 145–189. Reviews in Mineralogy, Mineralogical Society of America, Chantilly, Virginia.

Hirschmann, M.M., Baker, M.B., and Stolper, E.M. (1998) The effect of alkalis on the silica content of mantle-derived melts. Geochimica et Cosmochimica Acta, 62, 883–902.

Holzheid, A., Palme, H., and Chakraborty, S.(1997) The activities of NiO, CoO, and FeO in silicate melts. Chemical Geology, 139, 21–38.

Lewis, R.D., Lofgren, G.E., Franzen, H.F., and Windom, K.E. (1993) The effect of Na vapor on the Na content of chondrules. Meteoritic, 28, 622–628.

Mysen, B.O. and Frantz, J.D. (1993) Structure and properties of alkali silicate melts at magmatic temperatures. European Journal of Mineralogy, 5, 393–407.

O'Neill, H.St.C. (2005) A method for controlling alkali-metal oxide activities in one-atmosphere experiments and its application to measuring the relative activity coefficients of $NaO_{0.5}$ in silicate melts. American Mineralogist, 90, 497–501.

O'Neill, H.St.C. and Eggins, S.M. (2002) The effect of melt composition on trace element partitioning: an experimental investigation of the activity coefficients of FeO, NiO, CoO, MoO_2, and MoO_3 in silicate melts. Chemical Geology, 186, 151–181.

O'Neill, H.St.C., Pownceby, M.I., and McCammon, C.A. (2003) The magnesiowüstite-iron equilibrium and its implications for the activity-composition relations of $(Mg, Fe)_2SiO_4$ olivine solid solutions. Contributions to Mineralogy and Petrology, 146, 308–325.

Paul, A. and Douglas, R.W. (1965) Ferrous-ferric equilibrium in binary alkali silicate glasses. Physics and Chemistry of Glasses, 6, 207–211.

Pretorius, E.B. and Muan, A. (1992) Activity of nickel (II) oxide in silicate melts. Journal of the American Ceramic Society, 75, 1490–1496.

Ryerson, F.J. (1985) Oxide solution mechanisms in silicate melts: Systematic variations in the activity coefficients of SiO_2. Geochimica et Cosmochimica Acta, 49, 637–649.

Stebbins, J.F., McMillan, P.F., and Dingwell, D.B., Eds. (1995) Structure, dynamics and properties of silicate melts, 32. Reviews in Mineralogy, Mineralogical Society of America, Chantilly, Virginia.

Takahashi, E. (1978) Partitioning of Ni^{2+}, Co^{2+}, Fe^{2+}, Mn^{2+}, and Mg^{2+} between olivine and silicate melts: compositional dependence of partition coefficient. Geochimica et Cosmochimica Acta, 42, 1829–1844.

Tsuchiyama, A., Nagahara, H., and Hushiro, I. (1981) Volatilization of sodium from silicate melt spheres and its application to the formation of chondrules. Geochimica et Cosmochimica Acta, 45, 1357–1367.

MANUSCRIPT RECEIVED MAY 3, 2005
MANUSCRIPT ACCEPTED DECEMBER 16, 2005
MANUSCRIPT HANDLED BY DONALD DINGWELL